Phosphorous-doping in silicon nanocrystals

Naoki Inaba [a], Yoshufumi Nakamine [a], Yoshishige Tsuchiya [a,b], Hiroshi Mizuta [a,b], Ken Uchida [a], Rui N. Pereira [c], Andre R. Stegner [c], Martin S. Brandt [c], Martin Stutzmann [c], and Shunri Oda [a]

[a] *Quantum Nanoelectronics Research Center and Department of Physical Electronics, Tokyo Institute of Technology, and JST-SORST, Tokyo 152-8552, Japan*
e-mail:soda@pe.titech.ac.jp
[b] *School of Electronics and Computer Science, University of Southampton, Southampton, UK*
[c] *Walter Schottky Institut, Technische Universität München, Zografou, 85748 Garching, Germany*

It has been discussed that doping of impurities in nanocrystals is quite different from that of bulk semiconductors [1,2]. Self-purification effects and the increase of donor ionization energy may result in the question about the effects of impurity doping on electron transport. On the other hand, only a single or a few impurity atoms may contribute a drastic change of conductivity from insulating to metallic behavior in a limited number of host atoms. Previously, phosphorous doping in silicon nanocrystals embedded in oxide matrices was reported [3]. Recently, electrically detected magnetic resonance (EDMR) study of silicon nanocrystals prepared by microwave plasma decomposition of silane was reported [4].

We have prepared mono-dispersed Si nanocrystals by VHF plasma decomposition of silane [5] and demonstrated their quantum dot characteristics such as single electron tunneling effects [6], high-efficiency visible photoluminescence [7] and ballistic-electron emission [8]. In this work, we discuss preparations of Si nanocrystals with various P concentrations and characterization of the effects of doping by TEM and EDMR.

Si nanocrystals were fabricated by VHF plasma decomposition of SiH_4 [5,8]. The flow rate of SiH_4 was 3 sccm and that of Ar was 90 sccm. P doping was performed in situ using PH_3 gas diluted to 1% with Ar gas. Figure 1 depicts TEM images of Si nanocrystals with various flow rates of PH_3/Ar. Si nanocrystals are spherical and twin-free single-crystal as shown by the lattice images. The surface amorphous layer is natural oxide formed after exposure to the air. The thickness of surface amorphous layer increases with increasing P-concentration and hence the size of crystal core decreases as is also shown in Figure 2. Incorporation of P atoms enhances oxidation rate [9]. In energy-dispersive X-ray spectra, K_α line of phosphorous was observed only from P-doped Si nanocrystals.

Figure 3 shows EDMR spectra of Si nanocrystal films with (a,b) and without (c) P-doping. For undoped samples, only a signal from Si dangling bonds (Si-db) is detected, while for P-doped samples, an additional resonance due to the hyperfine structure of ^{31}P in Si can be observed. This signal increases in intensity after etching of the sample in HF (5% wt.) (curve(b)). These experimental facts suggest that P atoms substitute to Si sites and are located in the core crystal rather than in the oxide. However the low field counterpart of the hf(^{31}P) is not found at the opposite side of the characteristic center of the P hyperfine structure at g=1.998, presumably because it is buried under the broad Si-db signal.

In order to distinguish between magnetic resonance from dangling bonds and the hyperfine structure of ^{31}P, whose recombination lifetimes can be different, we carried out phase shift EDMR measurements [10]. The result with the Si-db being minimal, is shown in Figure 4. The signals at 341.5 mT and 335.6 mT with a central g-value of 1.998 are the hyperfine structure of ^{31}P in Si. This observation clearly indicates a successful incorporation of P dopants on substitutional lattice sites. It is notable that hyperfine splitting width of 5.9 mT is larger than that of bulk Si, which is 4.2 mT. This effect is attributed to quantum confinement of donor electrons in Si nanocrystals.

[1] S. C. Erwin, et. al. Nature, 436, (2005) 91.
[2] D. V. Melnikov and J. R. Chelikowsky, Phys. Rev. Lett., 92 (2004) 046802.
[3] M. Fujii, et. al., Phys. Rev. Lett. 89 (2002) 206805.
[4] A. R. Stegner, M. Stutzmann et. al., Phys. Rev. Lett. 100 (2008) 026803.
[5] T. Ifuku, S. Oda et al., Jpn. J. Appl. Phys. 36 (1997) 4031.
[6] A. Dutta, S. Oda et al., Jpn. J. Appl. Phys. 39 (2000) 4647.
[7] K. Arai, S. Oda et al., Mat. Res. Soc. Symp. Proc., 664, (2001) A20.6.
[8] K. Nishiguchi, S. Oda et al., J. Appl. Phys. 92 (2002) ,2748.
[9] L.C. Ciacchi and M.C. Payne, Phys. Rev. Lett., 95 (2005) 196101.
[10] H. Dersch, et. al., Phys. Rev. B 28 (1983) 4678.

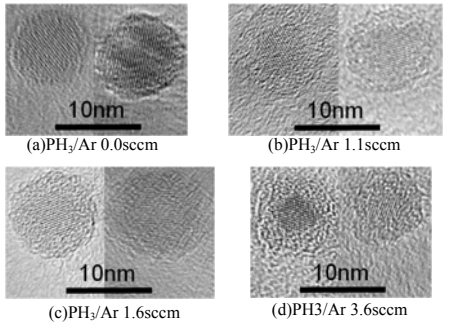

Figure 1. TEM images of surface oxidized silicon nanocrystals with various P concentrations.

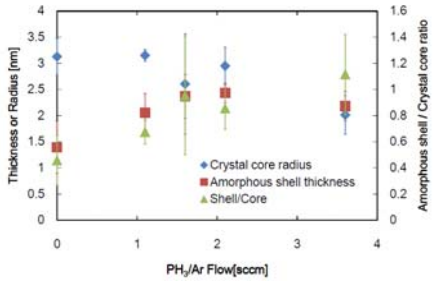

Figure 2. Crystal core size, oxide shell thickness and shell/core ratio with various P concentrations.

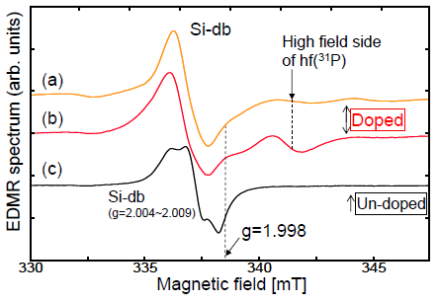

Figure 3. EDMR spectra from (a,b) P-doped and (c) undoped Si nanocrystals. Surface oxide was removed by HF for (b) and (c).

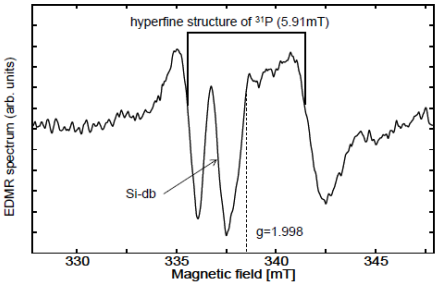

Figure 4. Phase shift EDMR spectrum from Si nanocrystals doped with P.